CHARMS: The Cryogenic, High-Accuracy Refraction Measuring System

B.J. Frey*, D.B. Leviton
NASA Goddard Space Flight Center, Greenbelt, MD 20771

ABSTRACT

The success of numerous upcoming NASA infrared (IR) missions will rely critically on accurate knowledge of the IR refractive indices of their constituent optical components at design operating temperatures. To satisfy the demand for such data, we have built a Cryogenic, High-Accuracy Refraction Measuring System (CHARMS), which, for typical IR materials, can measure the index of refraction accurate to $\pm 5 \times 10^{-5}$. This versatile, one-of-a-kind facility can also measure refractive index over a wide range of wavelengths, from 0.105 μm in the far-ultraviolet to 6 μm in the IR, and over a wide range of temperatures, from 10 K to 100°C, all with comparable accuracies. We first summarize the technical challenges we faced and engineering solutions we developed during the construction of CHARMS. Next we present our "first light," index of refraction data for fused silica and compare our data to previously published results.

1. INTRODUCTION

The optical designs of a wide variety of cryogenic, infrared optical instruments rely on transmissive, refracting optical materials. In order for the designs of these instruments to be optimal, practical, and feasible, it is essential to know the indices of refraction of the component materials to high accuracy. Furthermore, it is also desirable and often necessary to obtain index values for requisite materials at the actual temperatures and wavelengths of intended use.

Refractive index data already exists for a small subset of common IR optical materials – such as fused silica, silicon, germanium, zinc selenide, etc. – obtained at room temperature for shorter IR wavelengths. Meanwhile for high sensitivity IR instruments at longer wavelengths to work well, their optics must be cooled to cryogenic temperatures, often approaching absolute zero. Owing to limitations of conventional optical properties measurements and the cost and difficulty in building cryogenic measurement capabilities, high quality, IR refractive index data for longer wavelengths and at cryogenic temperatures, even for those common IR optical materials, is scarce. Data for less common yet still very useful materials, which open up optical design space, is altogether lacking.

Numerous NASA IR missions will require such accurate, cryogenic refractive index data for successful optical designs to be completed and instruments to be built. These missions and instruments include the James Webb Space Telescope (JWST), the Near Infrared Camera (NIRCam), the Fourier-Kelvin Stellar Interferometer (FKSI), the Space Infrared Interferometer Telescope (SPIRIT), the Sub-millimeter Probe of the Evolution of Cosmic Structure (SPECS), and the Earth Atmosphere Solar-occulting Imager (EASI), among others.

2. REFRACTOMETER SYSTEM ANATOMY

It is widely acknowledged that the most accurate and precise measurements of the real part of the refractive index, $n(\lambda,T)$, of optical materials are obtained through minimum deviation refractometry.[1,2] However, technical challenges have hindered researchers from using this technique in certain wavelength and temperature ranges, especially when moderately but adequately accurate data for given applications can be obtained through easier methods for those conditions. The initial design and development of CHARMS is documented in several other publications,[3,4,5] so here we only briefly review the system operation and concentrate on exploring the technical and engineering challenges that have shaped CHARMS.

* Bradley.J.Frey@nasa.gov, phone 1 301 286-7787, fax 1 301 286-0204, NASA Goddard Space Flight Center, Code 551, Greenbelt, MD, 20771

2.1 System overview: minimum deviation refractometry

CHARMS is a minimum deviation prism refractometer enclosed in a small, high-performance thermal vacuum chamber. The minimum deviation method of refractometry requires the precise and accurate knowledge of two angles: the apex angle, α, of a prismatic sample, and the deviation angle, δ, of the beam passing through the sample when the condition of minimum deviation is satisfied (see Figure 1). The condition of minimum deviation is established when the incident angle of an incoming (incident) ray is equal to that of the outgoing (deviated) ray; consequently, inside the prism the ray propagates perpendicular to the bisector of the apex. The difference between the direction of the undeviated ray and the direction of the deviated ray is the "deviation angle" through the prism; it can easily be shown using Snell's law that under these conditions the deviation angle is minimized and unique.

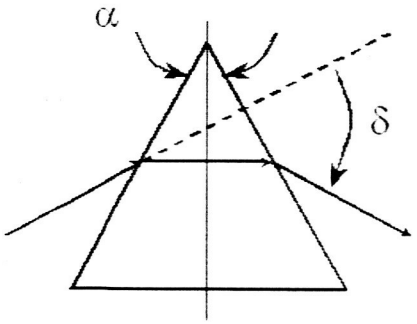

Figure 1: Required parameters in minimum deviation refractometry

2.2 Overview of system operation

To begin a set of refractive index measurements, we first mount the sample inside the sample chamber (see Figure 11, section 3.5), evacuate the system, and cool the sample to the desired temperature. We constantly monitor temperatures in the system during this process using silicon diodes and T-type thermocouples. There are several components in our system, however, whose survival rely on operation near room temperature (such as our ultra low runout mechanical spin tables); for these we can add heat as necessary through a network of kapton heaters. Once the sample reaches thermal equilibrium – roughly 8 hours for temperatures near 20 K – we select the appropriate starting wavelength and begin taking measurements.

Under automated control, the software rotates the first fold flat to steer the undeviated slit image to the reference (center) column on the detector array. The orientation of the fold flat rotary stage is recorded by the absolute encoders (see section 3.1) and saved in memory as the undeviated position. "Nulling" the slit image position on the detector array – i.e. requiring the deviated slit image centroid to land on this same detector reference column during subsequent angle measurements – enables the most accurate measurements of the deviation angle. Next, the software rotates the fold flat to the approximate angle at which it expects to find the deviated beam (as calculated from user inputs for best guess of index and nominal apex angle) and steers the deviated slit image onto the detector. Before nulling the deviated slit image to the center column, however, we must first orient the prism to satisfy the condition of minimum deviation (as described in section 2.1). The prism is rotated while the position of the deviated slit image centroid on the detector is recorded as a function of absolute rotary encoder angle on the sample platform. While the sample is continuously rotated in one direction, the deviated slit image on the detector moves in the direction of less deviation, stops, and then reverses direction as the prism is rotated through the condition of minimum deviation. Once the software completes that scan, the prism is returned to that orientation which provides minimum deviation (defined as the orientation at which the first derivative of slit image position on the detector versus prism rotation angle is zero), and the rotating fold flat now steers the refracted beam onto the previously defined reference column of the detector. The difference between the current encoder readings for the fold flat and the encoder readings for the undeviated beam is an angle which is exactly one-half of the deviation angle $\delta(\lambda,T)$ for that wavelength. (Because we are using a fold flat and not observing the slit image directly with a rotating camera arm, the angle through which the fold must be rotated to steer the slit image onto the reference column of the detector is only half of the actual deviation angle.) By measuring the directions of both deviated and undeviated beams for every data point – as opposed to measuring just the deviated beam and assuming the undeviated beam remains fixed – we can minimize errors associated with possible drifts in our system alignment.

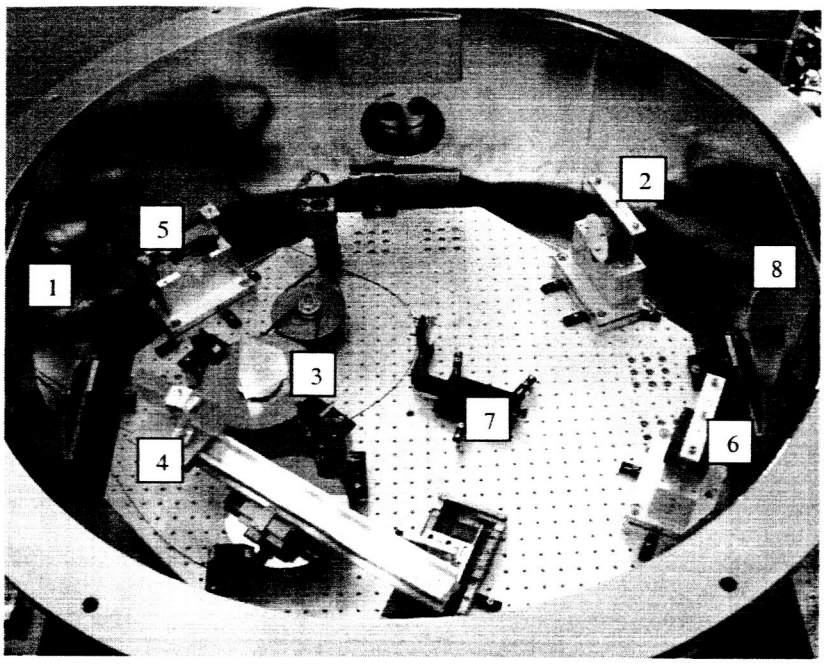

Figure 2: Current layout of CHARMS: (1) source (not shown), (2) collimating mirror, (3) sample prism, (4) rotating fold mirror, (5) fixed fold mirror, (6) camera mirror, (7) focus mirror, (8) detector (not shown).

The process is now repeated for all other wavelengths of interest while the temperature is held constant. (Actually, the temperature is held nearly constant but is very accurately measured, see section 3.5.) The only change in the procedure is that the condition of minimum deviation, having been found once, can be easily preserved as we change wavelengths, i.e. it does not need to be "found" for each new λ in the scan. Due to the symmetry of the angles of refraction at the prism faces with respect to the bisector of the prism's apex, the change in the angle of minimum deviation (defined as the position of the sample rotation stage which satisfies the conditions for minimum deviation) with wavelength is exactly equal to one half of the change in deviation angle. Since we are measuring the half-deviation angle as described in the preceding paragraph and not the deviation angle itself, this symmetry is manifest in a one-to-one correspondence between the change in deviation angle and the required rotation of the sample prism to maintain the condition of minimum deviation as we change wavelengths. In other words, if we rotate the sample prism by the same amount that we need to rotate the fold mirror to keep the deviated beam on the reference column of the detector as we change wavelengths, the condition of minimum deviation will be preserved.

Once the deviation angles for all wavelengths are measured for a given temperature, we are ready to measure the apex angle of the sample prism. Our ability to accurately measure the apex angle of the sample *in situ* as a function of temperature is yet another unique aspect of CHARMS. Rather than assuming that the apex angle remains constant through these potentially extreme thermal excursions, we are able to reduce our measurement uncertainty by determining the apex angle $\alpha(T)$ of the prism to an accuracy of better than ± 0.5 arcseconds for all temperatures. To do so, we make use of our recently developed electronic Cartesian autocollimator (CAC). The CAC is described more fully in section 3.2, and also in another paper.[6]

This completes a dataset for $n(\lambda,T)$ for one value of T. The same process is now repeated for each (λ,T) in the desired measurement parameter space. To gather the next data point, the software either allows the temperature to slowly drift up to the next desired temperature value, or it can add heat in the appropriate locations to drive the temperature of the sample to the next desired value. The actual value of the sample temperature is typically not of primary importance; rather, we insist only that the system be stable during the time needed to collect angle and temperature information for a single data point $n(\lambda,T)$. Since all of the appropriate parameters – T, $\alpha(T)$, and $\delta(\lambda,T)$ – are accurately measured during this time, we can safely *interpolate* between accurately measured data points to derive the index of refraction for

specific, yet arbitrary (λ,T). (This philosophy is to be contrasted with the less preferable but historical custom of *extrapolation* to arbitrary n(λ,T) from disparate wavelength and temperature regions). Finally we calculate the values of n(λ,T) according to the simple expression, unique to the condition of minimum deviation:

$$n(\lambda,T) = \sin\left(\frac{\alpha(T)+\delta(\lambda,T)}{2}\right)\Big/\sin\left(\frac{\alpha(T)}{2}\right).$$

3. ENGINEERING CHALLENGES AND INNOVATIONS

The primary reasons that high accuracy measurements of index such as these have not been made in the past stem from the number and variety of significant technical challenges involved. Many of these difficulties arise from working at cryogenic temperatures. Others are related to the precision metrology requirements required to make useful index measurements. Through a combination of novel engineering solutions and a design focused on attaining the highest accuracy measurements possible, we have been able to surmount or work around these challenges.

3.1 Precision rotations and their measurement

We would not be able to achieve our desired accuracy in CHARMS without the precision rotary stages and absolute optical encoders introduced in the previous section and pictured in Figure 3. Their unparalleled performance is essential for making the accurate and precise angular measurements required to build a refractometer capable of reporting refractive index accurately to the fifth decimal place. Our next challenge was to find a way to drive these stages that was compatible with our sub-arcsecond resolution requirement on rotation. Using a stepping motor, we drive the rotary stage by means of two pulleys and a custom designed, toothed gear that acts to decrease the step size of the motor to our desired resolution (see Figure 4a). We have improved upon this initial design by replacing the stepper motor in Figure 4a with the one pictured in Figure 4b. This new motor and motor controller give us better resolution and also the capability to change the fundamental motor step size and stepping rate through software to make our motions even more precise and efficient, respectively.

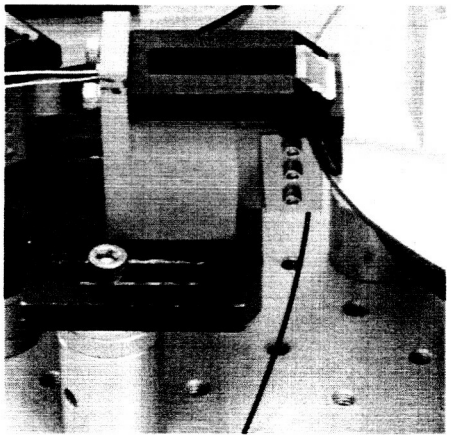

Figure 3a

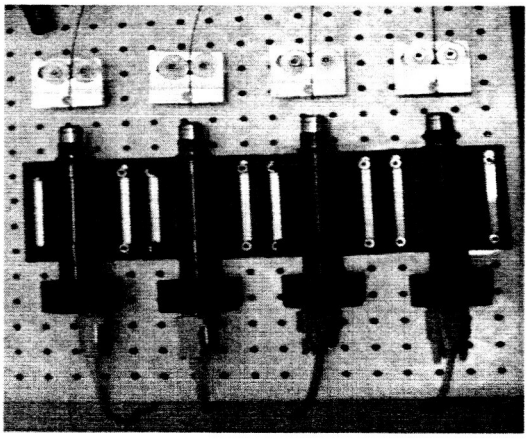

Figure 3b

Figure 3: Leviton absolute optical encoders: (3a) Encoder read head with 50K fiber image conduit. (3b) Encoder imaging electronics located external to thermal vacuum chamber.

3.2 Cartesian Autocollimator:

Just as the optical encoders allow us to make accurate determinations of the positions of the rotary stages, we need a way to accurately measure the apex angle of the sample prism, in place, as a function of temperature. In an attempt to simplify the measurement process, many previous refractometry efforts measured the apex angle of the prism under ambient conditions only, assuming the apex angle of the prism remained constant with temperature. This practice may be valid depending on the required index accuracy and on the type of material being measured. In order to meet our

index accuracy requirements, however, this assumption is unacceptably dangerous.

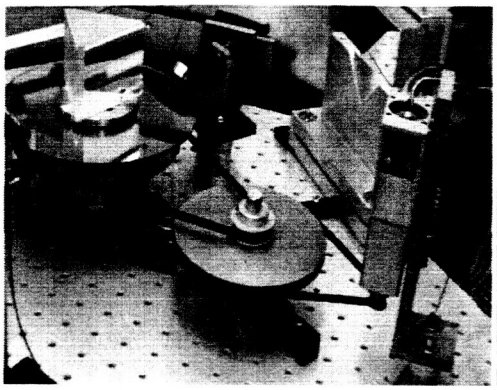

Figure 4a

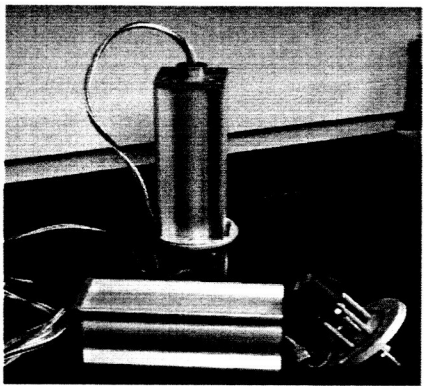

Figure 4b

Figure 4: (a) installed hardware for precision mechanical bearing and stepping motor drive mechanism (with gear reducer) for sample prism stage (b) hardware implementation of improved stepping motor packaging. The vacuum tight housing allows the stepping motor itself to operate in air while providing high precision rotary actuation inside the evacuated refractometer chamber

To meet our requirement to accurately measure apex angles as a function of temperature, we have developed an electronic autocollimator based on one of the new Leviton absolute Cartesian optical encoders. The inner workings of the Cartesian autocollimator (CAC) are discussed in another paper [6], but some results and the details of the present application are presented here. Apex angle measurements are taken once for each desired temperature of interest in the data set so that for each point T of $n(\lambda,T)$, we have a corresponding $\alpha(T)$. This method of measuring the apex angle of the prism is accurate to ±0.5 arcseconds, which limits its contribution to the overall error budget to 28×10^{-6} in knowledge of index for a typical sample prism in the IR.

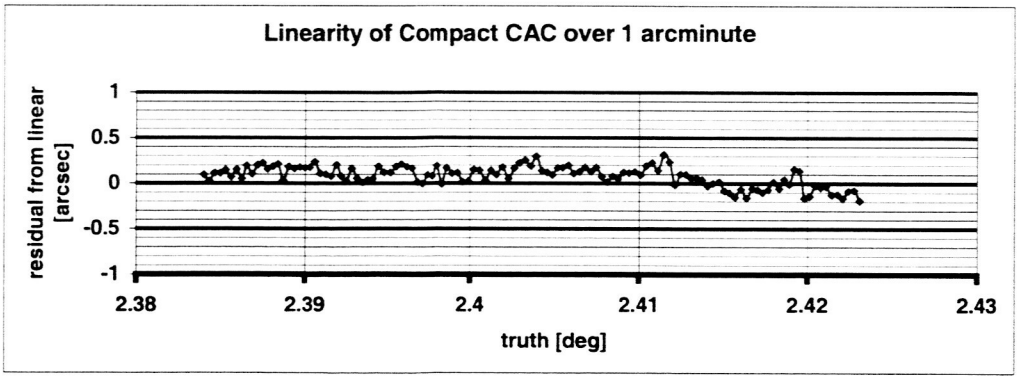

Figure 5: Sample data set showing agreement between CAC and absolute rotary optical encoders in air

3.3 Monochromator assembly and sources

Depending on the spectral dispersion, $dn/d\lambda$, for the material being measured, knowledge of wavelength may be one of the most significant sources of index uncertainty in our system. With this in mind, we are refurbishing a McPherson grating monochromator to satisfy our source wavelength accuracy requirements. Through combined exchanges of the light source and grating, we can use this versatile monochromator to realize a spectral range from 0.105 to 60 μm. To calibrate the monochromator readout as a function of wavelength, we will use several well-defined line sources across our available wavelength range to serve as fixed points in our calibration curve.

The monochromator stepping motor wavelength drive currently establishes a desired wavelength setting either by numeric command or by manually satisfying a mechanical counter setting. However, the accuracy of wavelengths set through this type of open loop control, i.e. with no actual position feedback, is less than ideal. In order to control wavelength output of the monochromator as accurately as possible, and to better than the manufacturer's specifications, we are exploring the addition of a Leviton rotary encoder (similar to encoders on the mechanical bearing stages) to the rotating shaft of the grating. By so doing, wavelength knowledge will actually be set in a closed-loop fashion as the actual measured angle of the grating's orientation corresponds directly to a wavelength calculated through the well-known grating equation.

3.4 Detector options and configurations

We have several different array-type detector options from which to choose depending on the wavelength range under study. For IR measurements we have purchased an Indigo Merlin camera that uses an indium antimonide (InSb) array detector having 320 x 256 pixels that are 30 μm square, cooled by a pour fill LN_2 dewar. By operating the Merlin in a windowless configuration, we anticipate a useful range of sensitivity from 1 to 6 μm. For coverage through the visible and into the UV, we have a windowless TI TC211 CCD having an array of 192 x 165 pixels that are 13.75 μm wide by 16 μm high. The CCD's surface is coated with a Lumigen phosphor to extend wavelength response down to around 120 nm in the FUV.

Regardless of the detector of choice, however, there are several detector parameters that contribute to our overall system accuracy. We rely on the ability to accurately centroid the refracted and undeviated slit images when making angular measurements with the absolute encoders that are at the heart of the refractometer. Depending on the element width of the detector array, the image width, and the signal-to-noise ratio of the peak of the image irradiance distribution, the centroid of the image can typically be determined to less than 0.005 element widths. For an element width of 30 μm and a plate scale of the camera mirror of 5 μm per arcsecond, the associated uncertainty is therefore 0.005 x 30 x 5 = 0.75 arcseconds. This uncertainty in knowledge of centroid position directly contributes to an uncertainty in the measured deviation angle for the sample prism and corresponds to an error in the amount of 20×10^{-6} in index. Averaging centroids will improve certainty, however, to a degree which is a yet to be determined.

3.5 Thermal system design and implementation

The design of the thermal system for CHARMS is entirely focused on getting the sample prism cold, isothermal, and stable. While we measure the index of refraction over a wide range of sample temperatures, we typically do not try to maintain the sample at any particular temperature. As explained in Section 2.1, it is only accurate and precise *knowledge* of temperature, not a particular value of the temperature, which is important for our measurements. The time constant associated with the passive drift in temperature for our system is such that we can sufficiently finely sample refractive index as a function of temperature to make valid interpolations between nearby data points to determine values of index for a particular temperature.

The first component of the thermal design is a cylindrical liquid nitrogen shroud lining the interior walls of the refractometer chamber. Next, we have designed a custom sample chamber that completely surrounds the sample, with the exception of two optical view ports where the incident and exit beams travel (see Figure 6). In addition to shielding the sample from any parasitic radiative heat loads, the sample chamber also acts to cool the sample conductively, as explained below. Using liquid cryogen or a cryogenic refrigerator to cool this sample chamber and, in turn, the sample, we can measure refractive index over a wide range of temperatures.

In order to conductively cool the sample, we rely on a series of high thermal conductivity braided copper straps (unfluxed desoldering braid) that couple the sample platform (upon which the sample sits) to the sample chamber. Taking into consideration the thermal conductivity of copper, the length and number of individual conductors in the braid, and the conductivity of the interfaces at either end of the braids, we determined that with 16 straps it would take 2 hours to cool the sample to 20 K; with 32 straps it might take as little as 1 hour. We currently plan to use 32 straps if we can empirically demonstrate that so many straps would not apply so much torque on the sample platform that the actual rotation angle of the sample would not track the rotation of the sample's rotation stage.

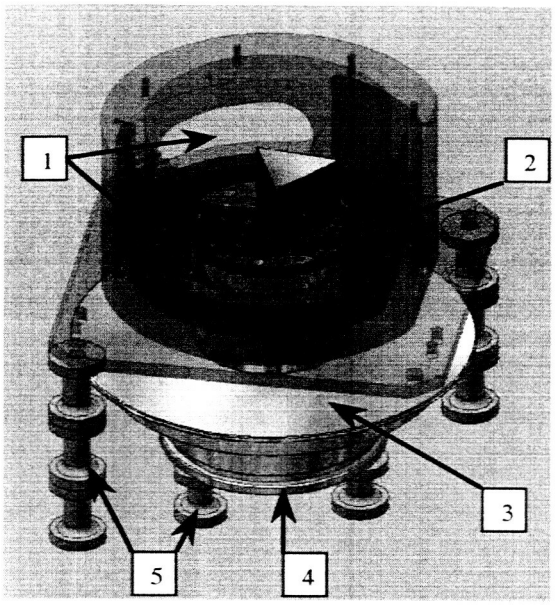

Figure 6: Windowless sample chamber with (1) optical viewports, (2) copper sample platform, (3) optical encoder scale, (4) mechanical bearing, and (5) G10 "thimble" isolators. Sample chamber is lid not shown.

4. ERROR ANALYSIS

Uncertainties in absolute index values by minimum deviation refractometry due to a number of environmental, optical, and mechanical sources have been derived elsewhere in the literature [2,7,8]. The goal in the design of the present refractometer is to attack every source of uncertainty with the aim of minimizing each for the most accurate data possible. For reference, we will first discuss potential sources of error and their respective weights in the overall error budget for a minimum deviation refractometer operating in the IR, and then we present our measured capabilities both in the IR and in the visible for two common prism materials.

4.1 Prism fabrication

Overall system accuracy begins with the specification of an appropriate prism size and apex for the best guess of index in the wavelength region of interest. Several different factors drive the requirements for fabrication of our sample prisms. We generally prefer to use a full 2.5 cm diameter refracted beam to maximize signal to noise in our centroiding algorithm. However, manufacturing a prism of that size is not always feasible. For example, to measure the index of a prism made of LiF with an approximate index of 1.38 at 2 μm and an optimal apex angle of 60°, we would need to have 3.8 cm long refracting faces at least 2.5 cm high to refract a beam 2.5 cm in projection; this may drive the cost of fabrication of a prism for that particular material to an unreasonable amount. Reducing the apex angle to 30° and making the refracting faces smaller may make the prism easier and less expensive to manufacture, but would nearly triple the uncertainty in deviation angle measurements and increase the uncertainty in apex by 50%. While this compromise in index accuracy may be acceptable in some instances, it nevertheless needs to be taken into consideration when specifying an appropriate prism for fabrication. Generally there is an optimal apex angle for a given sample material (i.e. refractive index) and primary wavelength that minimizes the uncertainty in apex and deviation angle measurements for a given system capability.

4.2 Sources of uncertainty

If we were to measure the spectral index of refraction of a germanium prism having an approximate index of 4.2 at a wavelength of 2.5 μm and an apex angle of 17° (which has been optimized for Ge at 2.5 μm), each source of uncertainty listed in Table 1 would contribute an error in the amount of one part in the sixth decimal place of absolute index.[2]

Establishing and maintaining the condition of minimum deviation is important, but is generally so easily achieved that no uncertainty is listed in the following tables.

Table 1– Sources of uncertainty in absolute index giving $\Delta n = 1 \times 10^{-6}$ for a Ge prism of apex 17° and index ~4.2 at 2.5 μm

apex angle	± 0.018	arcsecond	
half-deviation angle	± 0.04	arcsecond	
level	+ 9	arcminute	
sample temperature	± 0.2	C	relative to standard temp. (15 C)
air temperature	± 0.6	C	relative to standard temp. (15 C)
atmos. pressure	± 1.9	mm Hg	relative to standard pressure (760 mm)
humidity	± 3	H_20 mm Hg	relative to dry air (0 mm)
wavelength	± 0.03	nm	

4.3 Accuracy capabilities

Through the advances described in the previous sections, we believe we can improve the quality of our measurements significantly over previous efforts. In addition, by working in a vacuum, we are immune to many environmental sources of uncertainty such as air temperature, atmospheric pressure, and humidity that significantly influence refractometry at ambient conditions. Table 2 lists the most significant index uncertainties based on the current capabilities of our system for the same sample treated in Table 1. Table 3 describes our accuracy capabilities for fused silica measured in the visible for which we present our "first light" data in the following section.

Table 2–Expected capabilities in the IR in vacuum and uncertainties in n x 10^{-6} for the same Ge prism described in Table 1.

	capability		$\Delta n \times 10^{-6}$
apex angle	± 0.5	arcsecond	28
half-deviation angle	± 1.5	arcsecond	40
level	+ 9	arcminute	1
sample temperature	± 0.5	C	3
wavelength	± 0.2	nm	6

Taking these uncertainties in quadrature, we anticipate typical uncertainty in index below 5 x 10^{-5} in index for ideal prismatic forms of this and other IR materials.

Table 3–Measured capabilities in the visible and uncertainties in n x 10^{-6} for fused silica prism of apex 60° and index ~1.45

	capability		$\Delta n \times 10^{-6}$
apex angle	± 0.5	arcsecond	2
half-deviation angle	± 0.75	arcsecond	5
level	+ 9	arcminute	1
sample temperature	± 0.5	C	5
wavelength	± 0.1	nm	4

Taking these uncertainties in quadrature, our measured accuracy capabilities are below 1 x 10^{-5} in index for fused silica measured in the visible.

5. INITIAL RESULTS

5.1 Results for fused silica

At the time of this writing, we have the capability to make index measurements only at ambient conditions. We are in the process of installing and characterizing the thermal control system and hope to have full cryogenic measurement capability by the Summer of 2004. Nevertheless, we have made index measurements at ambient on several standard sample materials as verification of our capabilities. Here, we present our index data for fused silica.

Table 4: Representative spectral index data for fused silica corrected to 20° C.

Wavelength (nm)	Measured index (corrected to 20° C)	Derived value (Malitson)
640.1	1.456820	1.456809
632.8	1.457008	1.457018
611.9	1.457649	1.457651
604.6	1.457889	1.457886
594.1	1.458229	1.458237
543.5	1.460199	1.460190

In Table 4 and Figure 7, we present our initial refractive index measurements on a fused silica prism of nominal apex angle 60° in the visible. For this sample, the index measurements were done at 25° C and then corrected to 20° C for comparison with *de facto* standards of index of refraction measured by I.H. Malitson at the National Bureau of Standards[9] in the 1960's. In addition to determining the spectral dispersion equation for the index of fused silica, Malitson also determined that the interspecimen variability of fused silica introduces an uncertainty of 2×10^{-5} in index in this wavelength regime.

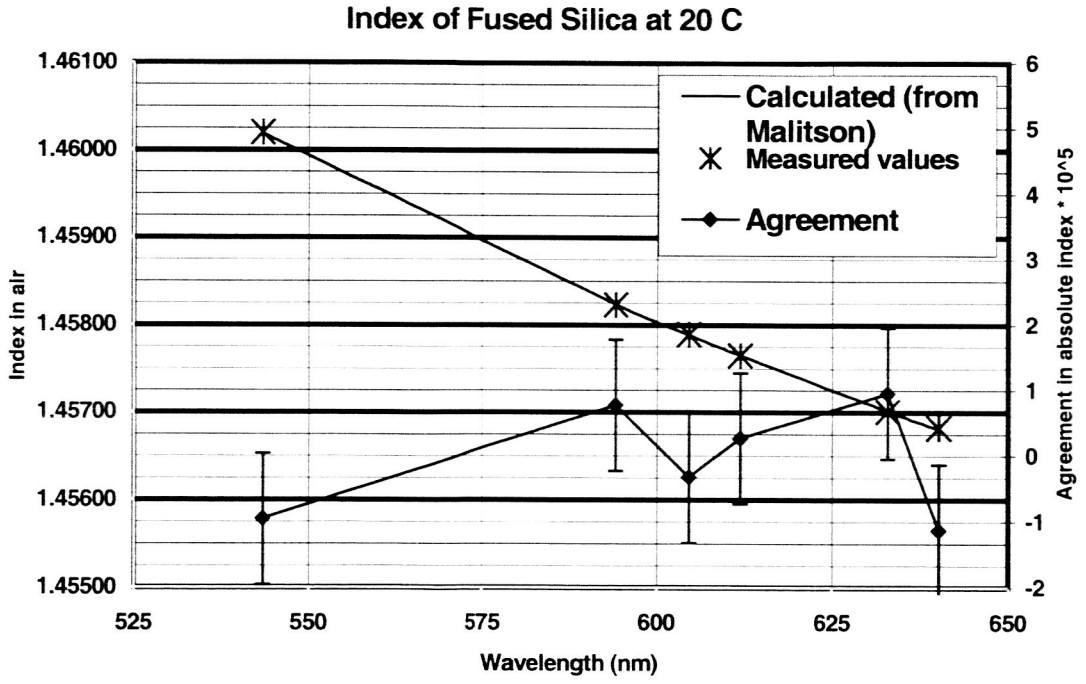

Figure 7: Calculated and measured spectral index of refraction of fused silica for selected wavelengths at 20° C.

For these initial measurements our setup was slightly modified from, but fundamentally very similar to, our final design. Though some components of the system were still being designed and fabricated, we wanted to make initial measurements to verify the operation of the hardware we did have and also to better understand the subtleties of the refractometer operation to improve the designs of those components that were not yet completed. The only significant change from our design was that in place of our grating monochromator, we chose to use a tunable helium-neon (HeNe) laser as our light source to illuminate a variable width slit. This gave us very accurate wavelength information and was easy to set up in place of our monochromator.

7. CONCLUSION

Several upcoming NASA missions and other industrial technologies using refractive optics will require accurate measurements of the index of refraction of their constituent optical components. While data do exist for some materials with limited accuracy over limited wavelength and temperature ranges, the overall availability of index of refraction data is largely insufficient. In an effort not only to provide increased accuracy of knowledge of the index of refraction for commonly used optical materials, especially in the infrared, but also to open up the available design space by measuring new and more exotic materials, we have built a minimum deviation prism refractometer with cryogenic measurement capabilities. This refractometer will improve upon the trusted methodology of minimum deviation refractometry by measuring both the deviation and apex angles of the prismatic sample for each temperature and wavelength of interest. We anticipate measurement capabilities from 0.120 μm in the far ultraviolet to 6 μm in the IR and at temperatures from near absolute zero to significantly above room temperature. Our anticipated level of accuracy is $\pm 1 \times 10^{-5}$ in absolute index in the visible and $\pm 5 \times 10^{-5}$ in the IR.

REFERENCES

1. D. Tentori, J.R. Lerma, "Refractometry by minimum deviation: accuracy analysis," Optical Engineering, **29**(2), pp. 160-168, February 1990
2. L.W. Tilton, "Prism refractometry and certain goniometrical requirements for precision," J. Res. of NBS, **2**, RP64, pp. 909-930, May 1929
3. D.B. Leviton, B.J. Frey, "Design of a cryogenic, high accuracy, absolute prism refractometer for infrared through far ultraviolet optical materials," SPIE **4842**, pp. 259-269, Waikoloa, August 2002
4. B.J. Frey, et. al., "Cryogenic high-accuracy absolute prism refractometer for infrared through far-ultraviolet optical materials: implementation and initial results," SPIE **5172-16**, San Diego, August 2003
5. D.B. Leviton, B.J. Frey, "Thermal design considerations for the cryogenic high accuracy refraction measuring system (CHARMS)" SPIE **5172-22**, San Diego, August 2003
6. D.B. Leviton, "Ultra-high resolution absolute Cartesian electronic autocollimator" SPIE **5190-53**, San Diego, August 2003
7. L.W. Tilton, "Standard conditions for precise prism refractometry," J. Res. of NBS, **14**, RP776, pp. 393-418, April 1935
8. L.W. Tilton, "Permissible curvature of prism surfaces and inaccuracy of collimation in precise minimum-deviation refractometry," J. Res. of NBS, **11**, RP575, pp.25-57, March 1933
9. I. H. Malitson, "Interspecimen comparison of the refractive index of fused silica," J. of the OSA, **55**(10), pp. 1205-1209, October 1965